

# Data report: hysteresis measurements on basalts from Holes U1346A, U1347A, and U1350A on Shatsky Rise<sup>1</sup>

Claire Carvallo<sup>2</sup>

## Chapter contents

<b>Abstract</b> .....	<b>1</b>
<b>Introduction</b> .....	<b>1</b>
<b>Methods and materials</b> .....	<b>2</b>
<b>Results</b> .....	<b>2</b>
<b>Acknowledgments</b> .....	<b>2</b>
<b>References</b> .....	<b>2</b>
<b>Figures</b> .....	<b>3</b>
<b>Tables</b> .....	<b>7</b>

## Abstract

I measured hysteresis loops and direct current backfield curves on 11 samples from Hole U1346A, 58 samples from Hole U1347A, and 51 samples from Hole U1350A, which were cored during Integrated Ocean Drilling Program Expedition 324 on Shatsky Rise. The hysteresis parameters of these samples showed a variety of values, mostly ranging from single-domain to pseudosingle-domain behaviors.

## Introduction

Shatsky Rise was cored during Integrated Ocean Drilling Program Expedition 324 because it is a unique oceanic plateau formed mainly during the Late Jurassic and Early Cretaceous at a rapidly spreading triple junction, with characteristics that could be attributed to either a plume or plate model of formation (Sager, 2005). Shatsky Rise is also a gigantic volcanic construct whose formation style is poorly understood. The goal of Expedition 324 was to core the igneous rock of Shatsky Rise and the sediment above to examine the age, physical volcanology, geochemistry, and tectonic evolution of the rise as well as the sedimentation history (Sager et al., 2010, 2011).

Thermal and alternating field (AF) demagnetizations were carried out by the shipboard paleomagnetists on discrete samples in order to give an estimate of the inclination of the recorded geomagnetic field. These shipboard results were reported in the Expedition Reports (see the “[Expedition 324 summary](#)” chapter [Expedition 324 Scientists, 2010]). In order to carry out more detailed paleomagnetic studies, more samples were collected as minicores for thermal and AF demagnetizations to be carried out in several laboratories on shore. Whenever possible, four or five samples were cut for each flow unit. To better understand the magnetic mineralogy of the sampled flows, I collected a slice of sample from the bottom of each minicore from Sites U1346, U1347, and U1350 for hysteresis measurements. Some results were presented in [Carvallo and Camps \(2013\)](#), but that study focused on a few lava flows that were selected for paleointensity study (Carvallo et al., 2013). Hysteresis measurements were subsequently made on the larger suite of samples and are presented here.

<sup>1</sup>Carvallo, C., 2014. Data report: hysteresis measurements on basalts from Holes U1346A, U1347A, and U1350A on Shatsky Rise. In Sager, W.W., Sano, T., Geldmacher, J., and the Expedition 324 Scientists, Proc. IODP, 324: Tokyo (Integrated Ocean Drilling Program Management International, Inc.).

doi:10.2204/iodp.proc.324.205.2014

<sup>2</sup>Institut de Minéralogie, de Physique des Matériaux et de Cosmochimie, Sorbonne Universités, UPMC Univ Paris 06, UMR CNRS 7590, Muséum National d’Histoire Naturelle, IRD UMR 206, 4 Place Jussieu, F-75005 Paris, France.  
[carvallo@impmc.upmc.fr](mailto:carvallo@impmc.upmc.fr)



## Methods and materials

Hysteresis measurements were carried out using an alternating gradient magnetometer at the Institut de Minéralogie, de Physique des Matériaux et de Cosmochimie, Université Pierre et Marie Curie (Paris, France). A millimeter-size chip was fixed on the probe with grease. A maximum field of 0.5 T was applied, and the averaging time was 100 ms, which was enough to obtain a good signal because the magnetization was strong enough. Hysteresis loops were corrected for the dia- and paramagnetic contribution, and the parameters  $M_r$  (remanent magnetization),  $M_s$  (saturation magnetization), and  $H_c$  (coercivity field) were calculated from the corrected loops. Backfield direct current curves were also measured for each sample in order to obtain the remanent coercivity field ( $H_{cr}$ ).

## Results

### Hole U1346A

Hysteresis curves were measured on 11 samples from Hole U1346A. Hysteresis parameters are listed in Table T1, and two examples of hysteresis loops are plotted on Figure F1.  $M_r/M_s$  ratios range from 0.190 to 0.401, and  $H_{cr}/H_c$  ratios range from 1.33 to 1.68. On a Day plot, these parameters place the samples just below the mixing single-domain (SD)–multidomain (MD) curve from Dunlop (2002) close to the values corresponding to ~20% MD or less (Fig. F2).

### Hole U1347A

Hysteresis curves were measured on 67 samples from Hole U1347A (including the samples studied in Carvallo and Camps, 2013). Hysteresis parameters are listed in Table T2, and examples of hysteresis loops are plotted on Figure F3. Two main behaviors can be identified. Most samples are pseudosingle-domain (PSD)-like, with  $M_r/M_s$  ratios between 0.096 and 0.350 and  $H_{cr}/H_c$  ratios between 1.30 and 5.00 (Fig. F3A). Among these samples, some seem to contain a small higher coercivity component (Fig. F3B). The other samples are characterized by  $M_r/M_s$  ratios close to 0.500, which is characteristic of SD magnetic carriers (Fig. F3C). On a Day plot, these parameters place most of the samples just below the mixing SD–MD curve from Dunlop (2002) close to the values corresponding to ~20% MD or less, but a few samples contain as much as 70% MD grains (Fig. F2).

### Hole U1350A

Hysteresis parameters were measured on 64 samples from Hole U1350A (including the samples studied in

Carvallo and Camps, 2013). Hysteresis parameters are listed in Table T3, and examples of hysteresis loops are plotted on Figure F4. Of the samples from this hole, 65% have  $M_r/M_s$  ratios between 0.100 and 0.250, which is fairly low; coercivities mostly lower than 10 mT; and  $H_{cr}/H_c$  ratios between 1.30 and 1.80 (Fig. F4A). Toward the bottom of the hole, samples have higher  $M_r/M_s$  ratios (Fig. F4B), ranging between 0.250 and 0.380, which seems to indicate a more SD behavior. In general, these parameters plot just below the SD–MD mixing line on the Day plot, with a composition between 20% and 50% MD grains (Fig. F2).

## Acknowledgments

This research used samples and data provided by Integrated Ocean Drilling Program (IODP). I thank W.W. Sager for his help with the manuscript, IODP for receipt of samples, and an anonymous reviewer for helpful comments.

## References

- Carvallo, C., and Camps, P., 2013. Data report: magnetic properties of basalts from Shatsky Rise. *In* Sager, W.W., Sano, T., Geldmacher, J., and the Expedition 324 Scientists, *Proc. IODP*, 324: Tokyo (Integrated Ocean Drilling Program Management International, Inc.). [doi:10.2204/iodp.proc.324.201.2013](https://doi.org/10.2204/iodp.proc.324.201.2013)
- Carvallo, C., Camps, P., Ooga, M., Fanjat, G., and Sager, W.W., 2013. Palaeointensity determinations and rock magnetic properties on basalts from Shatsky Rise: new evidence for a Mesozoic dipole low. *Geophys. J. Int.*, 192(3):986–999. [doi:10.1093/gji/ggs100](https://doi.org/10.1093/gji/ggs100)
- Dunlop, D.J., 2002. Theory and application of the Day plot ( $M_r/M_s$  versus  $H_{cr}/H_c$ ). 1. Theoretical curves and tests using titanomagnetite data. *J. Geophys. Res.: Solid Earth*, 107(B3):2056. [doi:10.1029/2001JB000486](https://doi.org/10.1029/2001JB000486)
- Expedition 324 Scientists, 2010. Expedition 324 summary. *In* Sager, W.W., Sano, T., Geldmacher, J., and the Expedition 324 Scientists, *Proc. IODP*, 324: Tokyo (Integrated Ocean Drilling Program Management International, Inc.). [doi:10.2204/iodp.proc.324.101.2010](https://doi.org/10.2204/iodp.proc.324.101.2010)
- Sager, W.W., Sano, T., and Geldmacher, J., 2011. How do oceanic plateaus form? Clues from drilling at Shatsky Rise. *Eos, Trans. Am. Geophys. Union*, 92(5):37–38. [doi:10.1029/2011EO050001](https://doi.org/10.1029/2011EO050001)

Initial receipt: 22 January 2014

Accepted: 12 March 2014

Publication: 5 May 2014

MS 324-205

**Figure F1.** Examples of representative hysteresis loops for two samples from Hole U1346A.  $M_r/M_s$  = remanent magnetization/saturation magnetization ratio,  $H_{cr}/H_c$  = remanent coercivity/coercivity field ratio. A. Sample 324-U1346A-7R-3, 49–51 cm. B. Sample 324-U1346A-11R-1, 97–99 cm.

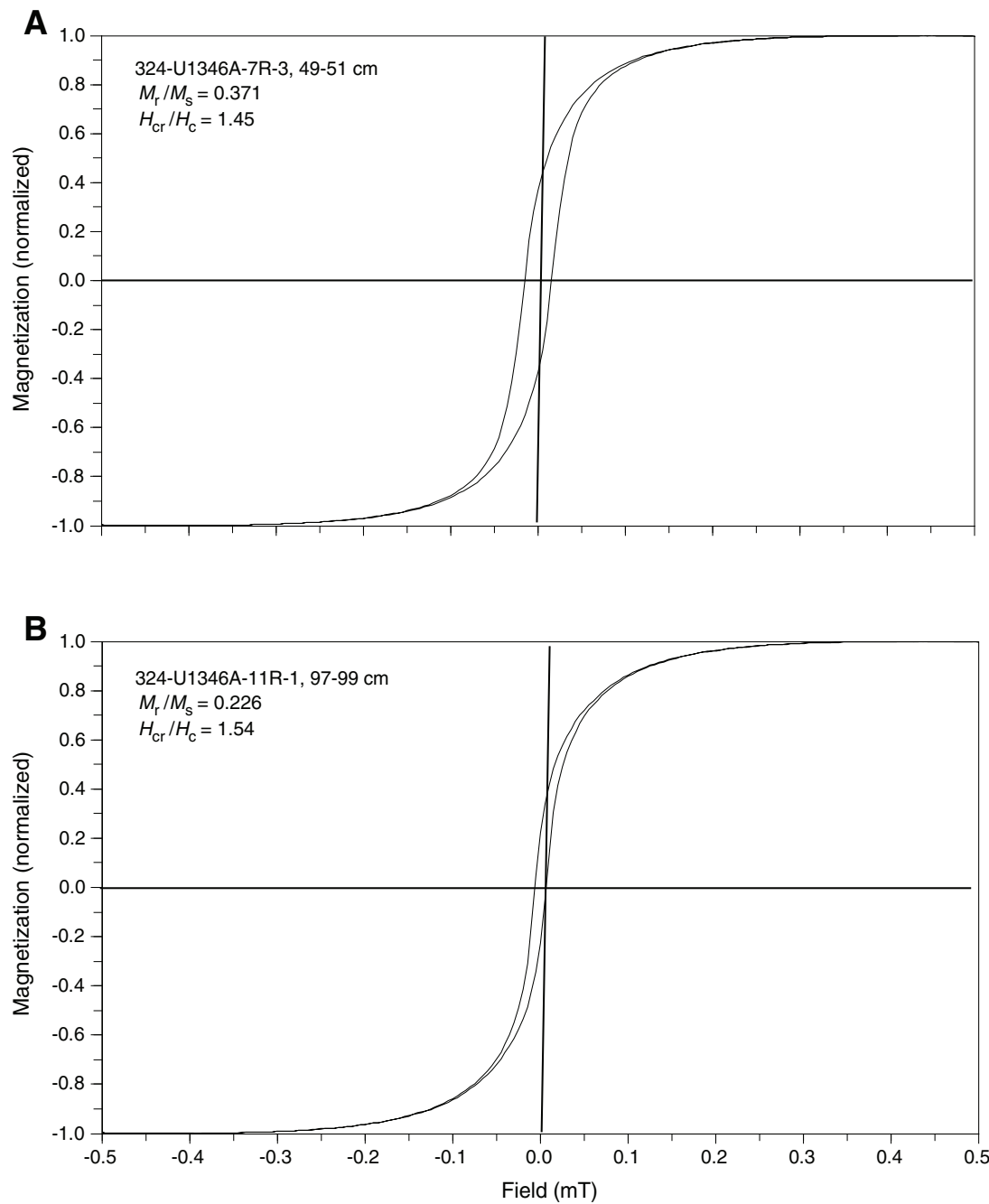


**Figure F2.** Day plot for the measured samples. The solid line is the single-domain (SD)–multidomain (MD) mixing line of Dunlop et al. (2006). Circled crosses = Hole U1346A, solid diamonds = Hole U1347A, open diamonds = Hole U1350A.  $M_r/M_s$  = remanent magnetization/saturation magnetization ratio,  $H_{cr}/H_c$  = remanent coercivity/coercivity field ratio.

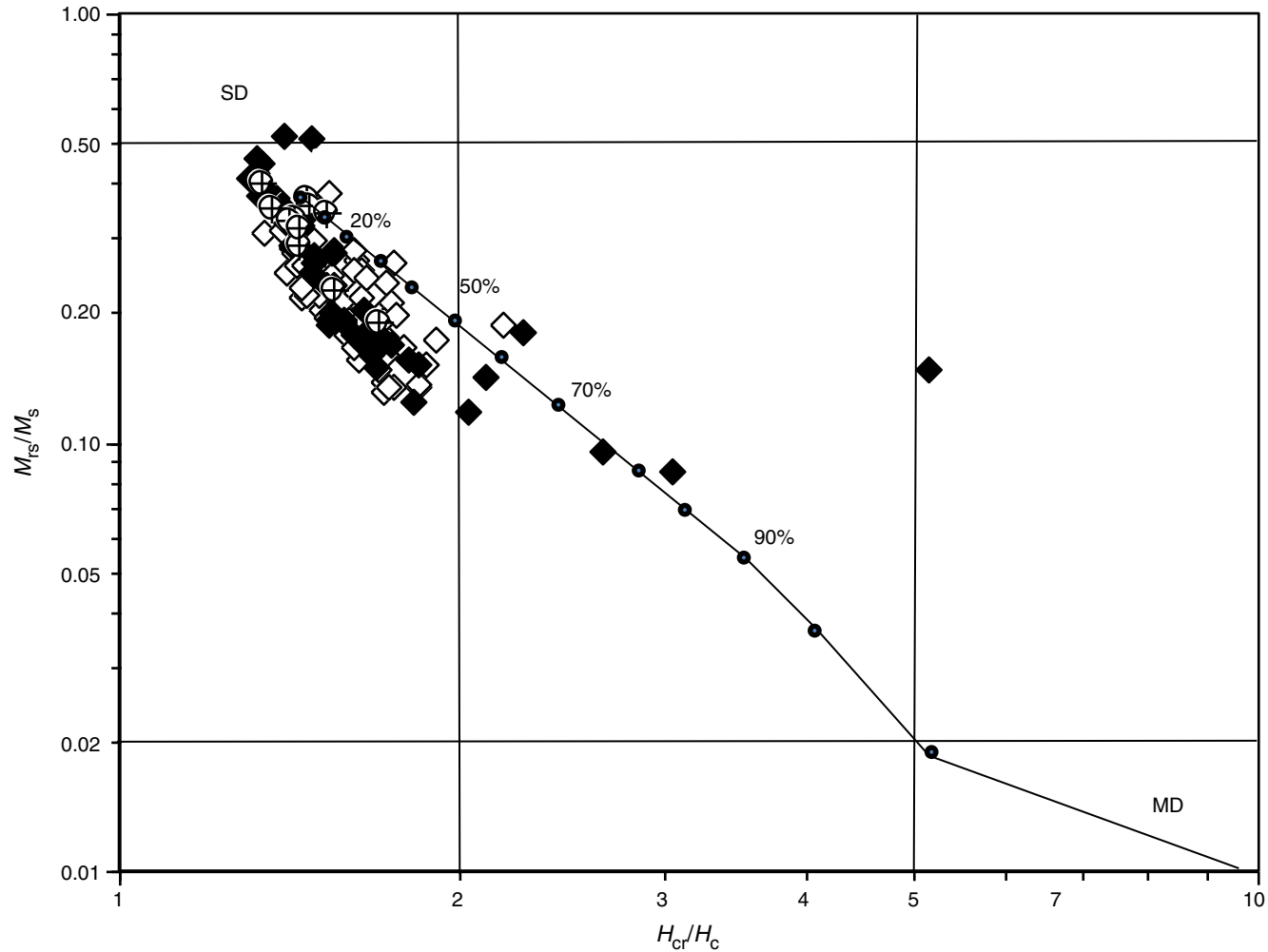


**Figure F3.** Examples of representative hysteresis loops for three samples from Hole U1347A.  $M_r/M_s$  = remanent magnetization/saturation magnetization ratio,  $H_{cr}/H_c$  = remanent coercivity/coercivity field ratio. A. Sample 324-U1347A-27R-3, 8–10 cm. B. Sample 324-U1347A-18R-3, 143–145 cm. C. Sample 324-U1347A-18R-4, 54–56 cm.

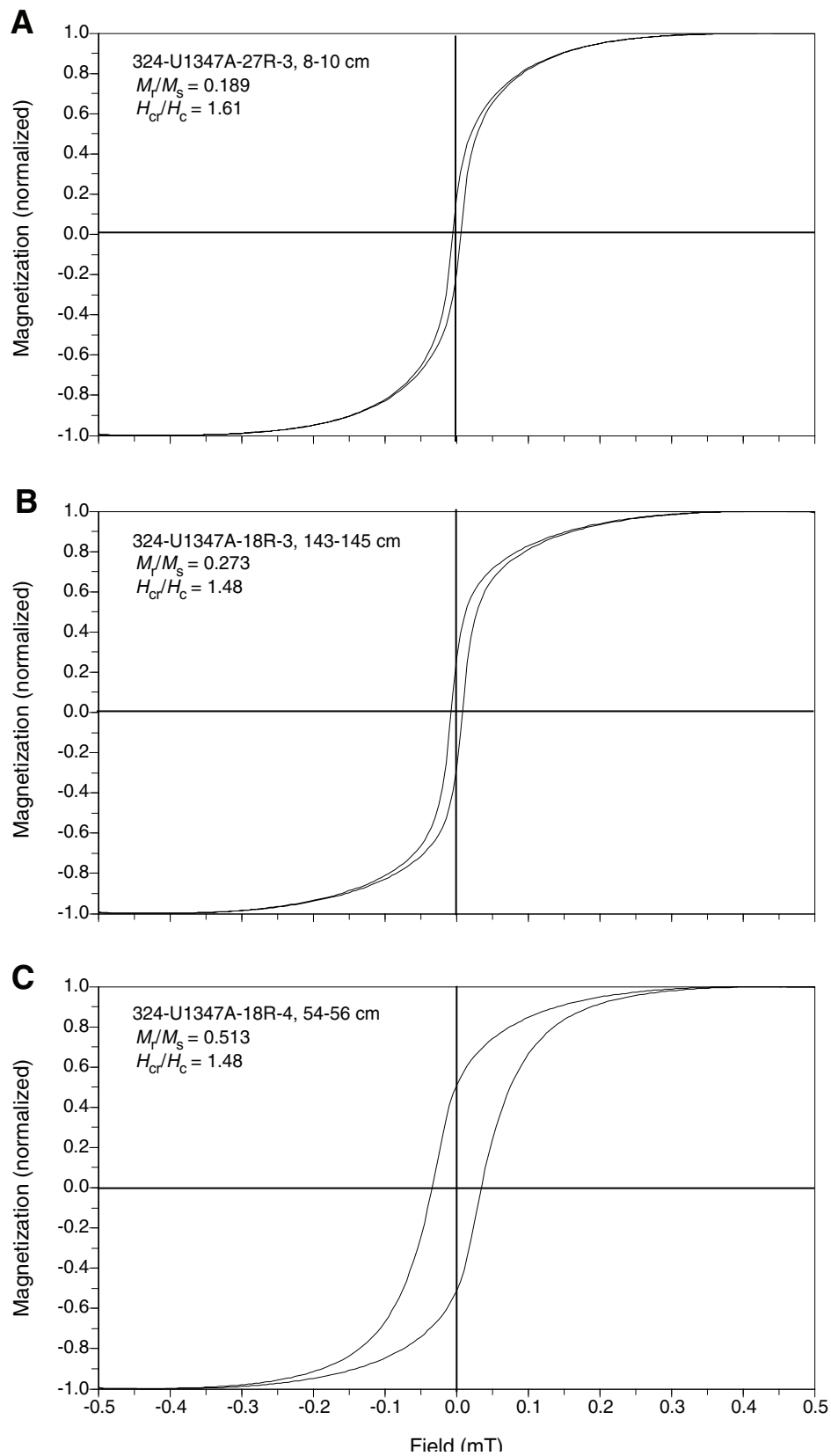


**Figure F4.** Examples of representative hysteresis loops for two samples from Hole U1350A.  $M_r/M_s$  = remanent magnetization/saturation magnetization ratio,  $H_{cr}/H_c$  = remanent coercivity/coercivity field ratio. A. Sample 324-U1350A-16R-3, 105–107 cm. B. Sample 324-U1350A-22R-2, 68–70 cm.

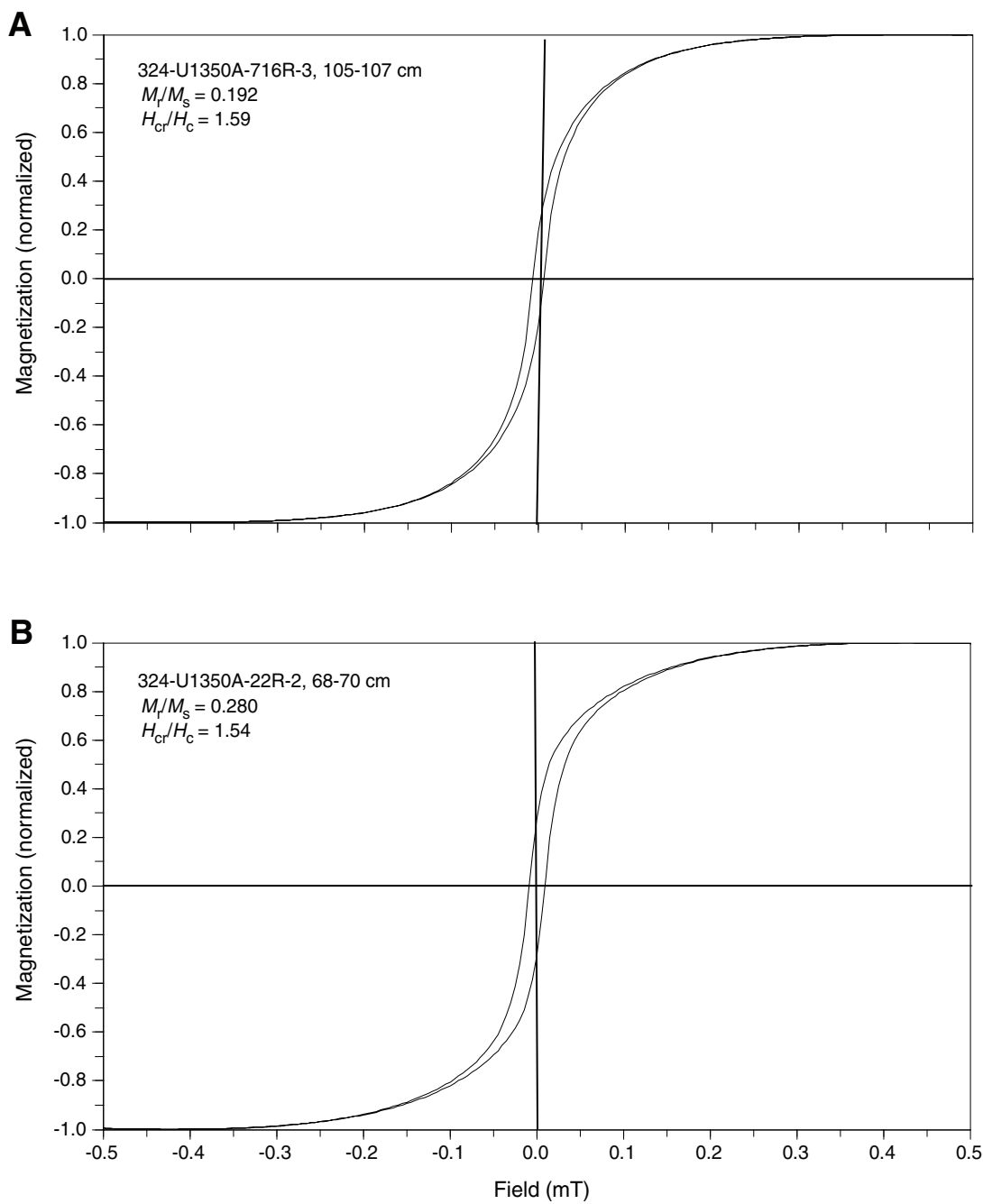


**Table T1.** Hysteresis parameters for samples from Hole U1346A.

Core, section, interval (cm)	$M_r/M_s$	$H_c$ (mT)	$H_{cr}$ (mT)	$H_{cr}/H_c$
324-U1346A-				
7R-3, 49–51	0.371	15.44	22.46	1.45
7R-4, 53–55	0.290	9.16	13.15	1.44
8R-1, 136–138	0.356	7.21	10.58	1.47
9R-1, 104–106	0.333	6.47	9.19	1.42
10R-1, 40–42	0.401	9.62	12.80	1.33
10R-2, 75–77	0.190	5.29	8.91	1.68
11R-1, 97–99	0.226	6.22	9.59	1.54
13R-2, 59–61	0.342	13.81	20.91	1.51
14R-1, 136–138	0.331	10.32	14.50	1.41
16R-1, 78–80	0.352	11.53	15.63	1.36
16R-2, 35–37	0.316	9.43	13.54	1.44

$M_r$  = remanent magnetization,  $M_s$  = saturation magnetization,  $H_c$  = coercive field,  $H_{cr}$  = remanent coercivity field.

**Table T2.** Hysteresis parameters for samples from Hole U1347A. (Continued on next page.)

Core, section, interval (cm)	$M_r/M_s$	$H_c$ (mT)	$H_{cr}$ (mT)	$H_{cr}/H_c$
324-U1347A-				
12R-1, 93–95	0.178	5.58	8.95	1.60
12R-1, 104–106	0.161	5.20	8.65	1.66
12R-2, 2–4	0.195	5.89	9.06	1.54
12R-2, 81–83	0.189	5.24	7.98	1.52
13R-1, 7–9	0.194	6.23	9.50	1.53
13R-2, 14–16	0.287	7.62	10.78	1.42
13R-3, 23–25	0.150	4.89	8.18	1.67
13R-6, 132–134	0.170	5.41	9.37	1.73
14R-1, 51–53	0.162	5.56	9.26	1.67
14R-1, 84–86	0.168	5.44	8.97	1.65
14R-2, 110–112	0.331	12.15	17.44	1.44
15R-2, 15–17	0.319	12.06	17.39	1.44
16R-1, 21–23	0.152	5.17	9.45	1.83
16R-2, 14–16	0.125	4.16	7.51	1.81
16R-3, 29–31	0.156	5.37	9.62	1.79
16R-5, 116–118	0.203	6.28	10.25	1.63
17R-2, 94–96	0.202	6.18	9.46	1.53
17R-3, 86–88	0.193	6.11	9.57	1.57
18R-3, 143–145	0.273	7.74	11.46	1.48
18R-4, 54–56	0.513	34.20	50.45	1.48
18R-5, 66–68	0.445	16.39	21.81	1.33
18R-6, 34–36	0.355	10.44	14.48	1.39
19R-1, 117–119	0.519	30.30	42.23	1.39
19R-2, 100–102	0.462	17.04	22.40	1.31
19R-3, 20–22	0.378	11.30	14.97	1.32
19R-4, 20–22	0.415	12.29	15.97	1.30
20R-1, 22–24	0.422	13.38	17.62	1.32
20R-2, 44–46	0.385	11.99	16.09	1.34
20R-3, 5–7	0.385	11.93	15.97	1.34
21R-4, 12–14	0.181	5.10	8.54	1.67
21R-5, 65–67	0.235	7.14	10.96	1.54
22R-1, 51–53	0.234	6.98	10.57	1.51
22R-2, 74–76	0.264	8.24	12.19	1.48
22R-5, 9–11	0.190	5.41	8.52	1.57
22R-5, 61–63	0.275	9.25	14.20	1.54
23R-2, 134–136	0.337	11.49	16.77	1.46
23R-3, 62–64	0.272	10.36	15.77	1.52
23R-4, 103–105	0.281	8.74	13.20	1.51
24R-3, 136–138	0.254	8.36	13.03	1.56
24R-5, 49–51	0.314	10.26	14.76	1.44
24R-6, 69–71	0.175	5.61	9.15	1.63
24R-8, 65–67	0.312	10.00	14.45	1.45
24R-8, 127–129	0.192	6.82	11.32	1.66
25R-1, 84–86	0.291	10.46	15.60	1.49



**Table T2 (continued).**

Core, section, interval (cm)	$M_r/M_s$	$H_c$ (mT)	$H_{cr}$ (mT)	$H_{cr}/H_c$
25R-4, 125–127	0.251	8.83	13.78	1.56
26R-1, 103–105	0.263	9.34	14.45	1.55
26R-2, 29–31	0.358	9.74	13.40	1.38
26R-2, 121–123	0.183	6.22	10.26	1.65
27R-1, 71–73	0.248	8.37	12.30	1.47
27R-2, 78–80	0.227	5.71	9.44	1.66
27R-3, 4–6	0.143	4.70	9.82	2.09
27R-3, 8–10	0.189	5.50	8.88	1.61
27R-3, 65–67	0.194	5.75	9.43	1.64
27R-4, 21–23	0.180	6.57	14.85	2.26
27R-5, 4–6	0.428	15.30	20.66	1.35
27R-5, 12–14	0.327	13.58	19.00	1.40
27R-5, 120–122	0.152	3.62	6.53	1.80
27R-5, 125–127	0.118	3.72	7.51	2.02
27R-6, 6–8	0.149	5.46	28.01	5.13
27R-6, 22–24	0.174	3.99	6.71	1.68
27R-6, 119–121	0.096	3.25	8.61	2.65
28R-1, 8–10	0.148	3.46	6.21	1.80
28R-1, 74–76	0.086	3.47	10.58	3.05
28R-2, 28–30	0.119	3.52	7.06	2.01
28R-7, 13–15	0.149	3.28	5.73	1.75
29R-3, 68–70	0.101	2.83	5.79	2.05
29R-5, 86–88	0.224	6.15	9.33	1.52

$M_r$  = remanent magnetization,  $M_s$  = saturation magnetization,  $H_c$  = coercive field,  $H_{cr}$  = remanent coercivity field. Parameters from [Carvallo and Camps \(2013\)](#) are included.

**Table T3.** Hysteresis parameters for samples from Hole U1350A.

Core, section, interval (cm)	$M_r/M_s$	$H_c$ (mT)	$H_{cr}$ (mT)	$H_{cr}/H_c$
324-U1350A-				
7R-1, 104–106	0.135	4.91	8.95	1.82
8R-1, 63–65	0.137	4.82	8.83	1.83
8R-2, 4–6	0.208	7.43	11.76	1.58
8R-3, 4–6	0.179	5.25	8.29	1.58
9R-1, 58–60	0.162	4.75	7.71	1.62
9R-5, 9–11	0.138	4.71	8.02	1.70
11R-1, 128–130	0.223	6.15	9.01	1.46
11R-2, 14–16	0.131	4.16	7.09	1.70
13R-1, 100–102	0.212	5.86	9.01	1.54
13R-2, 55–57	0.180	4.87	7.55	1.55
14R-1, 52–54	0.203	5.35	8.04	1.50
15R-1, 101–103	0.135	3.74	6.50	1.74
16R-2, 5–7	0.227	7.43	11.26	1.52
16R-3, 105–107	0.192	6.21	9.89	1.59
17R-1, 138–140	0.160	5.56	9.52	1.71
18R-1, 72–74	0.217	5.60	8.08	1.44
18R-2, 73–75	0.156	5.23	8.48	1.62
19R-1, 119–121	0.212	7.27	11.34	1.56
19R-2, 125–127	0.149	4.41	7.43	1.68
20R-1, 65–67	0.222	6.35	9.49	1.50
20R-1, 95–97	0.249	6.41	8.98	1.40
20R-2, 67–69	0.136	4.34	7.45	1.72
20R-2, 132–134	0.197	5.38	8.18	1.52
21R-1, 23–25	0.168	5.34	8.55	1.60
21R-1, 137–139	0.220	6.37	9.28	1.46
21R-2, 135–137	0.309	9.20	12.33	1.34
21R-3, 64–66	0.193	6.02	9.56	1.59
22R-2, 67–69	0.229	6.44	9.29	1.44
22R-2, 68–70	0.280	8.81	13.56	1.54
22R-4, 87–89	0.225	7.13	11.49	1.61
22R-5, 71–73	0.176	6.07	10.40	1.71
22R-5, 135–137	0.213	7.55	13.09	1.73
23R-1, 22–24	0.152	5.58	10.33	1.85
23R-3, 125–127	0.166	5.76	10.22	1.78
23R-4, 16–18	0.268	9.57	15.40	1.61
23R-5, 6–8	0.381	21.64	32.97	1.52
24R-1, 42–44	0.275	10.15	16.21	1.60
24R-1, 111–113	0.263	12.56	21.85	1.74
24R-2, 137–139	0.281	10.26	16.44	1.60
24R-3, 27–29	0.222	8.15	13.61	1.67
25R-1, 61–63	0.218	7.56	12.32	1.63
25R-1, 102–104	0.267	7.47	10.94	1.47
25R-1, 112–114	0.257	7.59	11.05	1.46
25R-2, 60–62	0.311	9.68	13.39	1.38
25R-2, 64–66	0.253	9.21	15.01	1.63
25R-3, 80–82	0.245	8.96	13.71	1.53
25R-3, 83–85	0.281	8.02	11.54	1.44
25R-5, 92–94	0.256	7.29	10.70	1.47
25R-6, 31–33	0.284	8.26	11.94	1.44
25R-7, 5–7	0.235	7.83	13.39	1.71
25R-7, 91–93	0.284	7.97	11.29	1.42
25R-8, 13–15	0.372	14.21	19.52	1.37
26R-1, 28–30	0.295	10.02	14.81	1.48
26R-2, 12–14	0.254	9.35	14.96	1.60
26R-2, 40–42	0.277	7.86	11.15	1.42
26R-3, 6–8	0.276	9.44	14.44	1.53
26R-4, 39–41	0.194	6.00	10.20	1.70
26R-4, 89–91	0.173	6.83	12.91	1.89
26R-6, 12–14	0.252	7.02	10.42	1.48
26R-6, 80–82	0.198	7.09	12.41	1.75
26R-7, 13–15	0.260	7.12	10.18	1.43
26R-7, 9–11	0.189	6.00	13.00	2.17
26R-7, 96–98	0.241	9.62	15.78	1.64
26R-8, 43–45	0.259	7.61	11.05	1.45

$M_r$  = remanent magnetization,  $M_s$  = saturation magnetization,  $H_c$  = coercive field,  $H_{cr}$  = remanent coercivity field. Parameters from [Carvallo and Camps \(2013\)](#) are included.

